Journal Pre-proof

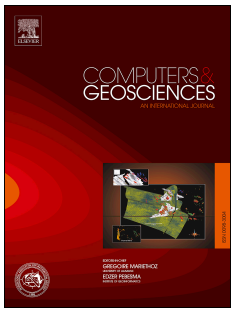

Image based Particle Shape Analysis Toolbox (IPSAT)

Mohit Tunwal, Kieran F. Mulchrone, Patrick A. Meere

PII: S0098-3004(19)30577-1

DOI: https://doi.org/10.1016/j.cageo.2019.104391

Reference: CAGEO 104391

To appear in: *Computers and Geosciences*

Received Date: 10 June 2019

Revised Date: 22 November 2019

Accepted Date: 24 November 2019

Please cite this article as: Tunwal, M., Mulchrone, K.F., Meere, P.A., Image based Particle Shape Analysis Toolbox (IPSAT), *Computers and Geosciences* (2019), doi: https://doi.org/10.1016/j.cageo.2019.104391.

Image based Particle Shape Analysis Toolbox (IPSAT)

Mohit Tunwal[1)2)*], *Kieran F. Mulchrone*[2)] *and Patrick A. Meere*[1)]

[1)] *School of Biological, Earth and Environmental Sciences, University College Cork, Distillery Fields, North Mall, Cork, T23 TK30, Ireland*

[2)]*School of Mathematical Sciences, University College Cork, Western Gateway Building, Western Road, Cork, T12 XF62, Ireland*

***Corresponding Author:** Mohit Tunwal[1]

Contact: mohittunwal@gmail.com; mohit.tunwal@ucc.ie; +353-21-490-4580

Link to code: https://github.com/tunwalm/IPSAT

Highights:

- Image analysis toolbox for particle shape and size analysis is presented
- 12 shape and 6 size parameters are available in the toolbox
- 2D to 3D size transformation & data visualisation tools are present in the toolbox
- Methodology for both loose as well as compacted samples is proposed
- Toolbox offers a cheap, fast and robust method for quantitative textural analysis

[11] Authorship Statement: MT and KFM developed the code. MT, KFM and PAM conceptualised the study as well as contributed to drafting the manuscript.

Abstract

Shape analysis can provide vital information regarding the origin, transport and deposition history of grains. Particle shape measurement has been an active area of research for sedimentologists since the 20th century. With advancement in the field of computation and image analysis, shape analysis can be done in a faster and much more accurate way compared to manual measurements. The results obtained are reproducible as compared to visual qualitative analysis. However, there is a lack of image analysis software tools aimed at the field of sedimentology where the fine details of a particle boundaries are required. Image based Particle Shape Analysis Toolbox (IPSAT) developed in the Mathematica environment for the quantitative characterisation of sedimentary grains in 2-dimensions is presented here. This image analysis toolbox can be used to analyse consolidated as well as loose sediment samples. A total of 12 parameters are available for shape measurement comprising conventional shape parameters (roundness, angularity, circularity and irregularity), mathematically complex shape parameters (fractal dimension and Fourier descriptors) and common geometrical shape parameters (aspect ratio, convexity, solidity, mod ratio, rectangularity and compactness). Additionally, IPSAT offers to compute 6 particle size measurement parameters. Furthermore, 2-D particle size distribution can be transformed to a 3-D size distribution for thin section analysis. Example analyses have been carried out on a sandstone and a loose sediment sample. The toolbox presented here aims to establish a textural analysis methodology to be used by geologists and sedimentologists in particular. It will allow users to quantitatively characterise a large set of grains with a fast, cheap and robust methodology.

Keywords: particle shape, particle size, image analysis, texture, roundness, angularity

1. Introduction

Particle shape analysis is of interest to a wide range of fields in geology such as igneous and metamorphic petrology (Higgins, 2006), structural geology (Heilbronner and Barrett, 2014; Mulchrone et al., 2013), volcanology (Charpentier et al., 2013; Sarocchi et al., 2011), and sedimentology (Blott and Pye, 2008). Shape analysis of sedimentary particles has occupied sedimentologists for over a century (Barrett, 1980; Blott and Pye, 2008 and references therein) as it provides vital information regarding the origin, transport and deposition history (Pettijohn, 1957). However, shape analysis studies suffer from two common shortcomings: 1) with a plethora of available shape parameters, a standardised methodology is lacking; 2) most of these shape parameters are time consuming and tedious to calculate manually. Visual comparison charts were proposed to ease the effort required for shape analysis (Krumbein, 1941; Powers, 1953). However, qualitative comparison methods suffer from user bias and reproducibility issues (Blatt, 1992; Blatt et al., 1972).

In recent years, with the advancement of computational power and image analysis techniques, shape analysis has received a renewed focus (Campaña et al., 2016; Moreno Chávez et al., 2018; Eamer et al., 2017; Lira and Pina, 2009; Sochan et al., 2015; Suzuki et al., 2015; Tao et al., 2018). Most of these methods have been primarily applied to loose sediments where it is easier to define grain boundaries automatically. On the other hand, the currently available automated grain boundary segmentation algorithms (Calderon De Anda et al., 2005; Gorsevski et al., 2012; Li et al., 2008; Mingireanov Filho et al., 2013; Roy Choudhury et al., 2006) do not produce the quality of grain boundary data from thin section microphotographs typically required for shape analysis. A high resolution microphotograph with clear distinction between matrix and clasts is

usually required (Roduit, 2007) for such automated grain boundary segmentation but this is the exception rather than the rule.

Another shortcoming in presently available image analysis tools is that they do not offer a wide range of shape parameters for a comprehensive shape analysis study. One of the most widely used image analysis software platforms, ImageJ, was developed primarily for use by biologists (Schneider et al., 2012). Hence, the *shape descriptors* present are basic geometrical shape measures related to overall macro features of the particle shape rather than a detailed characterisation of the particle outline as required for example for roundness measurement. Furthermore, recently proposed shape parameters by various researchers are either conceptual (Takashimizu and Iiyoshi, 2016) or are presented in standalone software (Charpentier et al., 2013; Heilbronner and Barrett, 2014).

The aim of this contribution is to present Image based Particle Shape Analysis Toolbox (IPSAT) – an image analysis software package that offers a wide range of shape and size parameters. IPSAT can used to quantitatively analyse particles from both loose sediments and rock thin section microphotographs. In the case of loose sediments, a fully automated approach is presented. On the other hand, manual tracing of grain boundaries is suggested for thin section photomicrographs. IPSAT is developed on the Mathematica platform which offers a variety of in-built powerful image analysis and computational routines.

The implementation details of the software code along with details of textural parameters are described in the next section. Example analyses for both loose and consolidated sediments are provided. The image analysis toolbox presented in this paper aims to establish a methodology for reproducible and comparable quantitative textural analysis of particles.

2. Software description

Mathematica is used as the basis for IPSAT and is a powerful technical computing environment with an excellent array of features and applications that run on a variety of operating systems such as Windows, Mac OS and Linux (Trott, 2013; Wellin et al., 2005). The IPSAT code is wrapped up in a single Mathematica package. Additionally, two example Mathematica notebooks are provided demonstrating the analysis of a thin section and a loose sediment sample. These notebooks guide the user though the procedure, i.e. from image import to image analysis, feature extraction, and computation of all the textural parameters. Furthermore, a detailed user manual is also included which provides step-by-step guide for usage of functions described in this section. The functionality of IPSAT package is summarised in Figure 1, the implementation details of which are as follows:

2.1. Image input and analysis

If a sample of unconsolidated (loose) sediment is to be analysed, then the process is much simpler and fully automated. Particles are recommended to be setup on the stage such that they do not touch each other (see Fig. 2a). In case of image from transmitted light, the background is expected to be light coloured with exceptions of dark region(s) representing particle(s). On the other hand, a black background with contrasting light coloured region(s) containing particle(s) is recommended for reflected light source image. The input image for loose sediment can be of any standard image format (e.g., JPEG, TIFF, PNG).

In the case of particles from lithified samples such as sandstone, photomicrographs of thin sections are used. Manual tracing of particle boundaries is performed because automated image analysis techniques are not yet satisfactory (Moreno Chávez et al., 2015; Gorsevski et al., 2012;

Li et al., 2008; Mingireanov Filho et al., 2013; Roy Choudhury et al., 2006). It is recommended that tracing paper and black inking pens are used for tracing (Mulchrone et al., 2013) or, alternatively, a graphics tablets may be used. Images consisting of black boundaries on a white background are the required input for the software (see Fig. 3b). A bitmap file (BMP) is recommended to be used as input for the manually traced image. Further details on image acquisition is provided in the Example Analysis (see section 3).

The **GrainBoundary** function is present only in the loose sediment analysis notebook. It detects the particle boundary using a threshold which can be changed, if required, by the user. The output of this step generates an image similar to a manually traced image (see Fig. 2b). All subsequent steps are same for both loose sediment and thin section image analysis.

Two functions (**GrabImage** and **RefineImage)** are written for image analysis purposes. The **GrabImage** function directly takes manually traced input image in the case of thin section analysis. For loose sediment analysis, the output of **GrainBoundary** is used as the input for the **GrabImage** function. **GrabImage** performs the following tasks:

(i) converts the input image into a binary image

(ii) generates a matrix by applying the watershed transformation on the image from step (i), at this stage all the particles are separately identified

(iii) using the built-in Mathematica function (ComponentMeasurement), all the initial geometric information regarding the grains are computed – long and short axis of best fit ellipse, orientation, centroid, area, convex area, perimeter and convex perimeter.

After the **GrabImage** function runs, it outputs a colourised image displaying individual particle regions in different colours with a unique label number (see Fig. 2c and 3c). Erroneous

identifications may remain at this point, where boundaries of neighbouring particles meet and form a closed loop.

RefineImage is a function allowing users to remove any erroneously identified regions. It accepts as an argument a list of the labels of unacceptable particles and removes them from further processing. Once RefineImage is run, a revised colourised image of identified particle regions is presented. This step may be repeated until the user is satisfied with the output.

2.2. Feature extraction

After the image analysis, the dataset is extracted from the image using the function **ExtractData**. This function extracts the coordinates of all the points lying on boundary, all the points lying inside the boundary and the relevant geometric data generated from GrabImage function (from task (iii)). The ExtractData function utilises in-built Mathematica functions to perform these tasks, for e.g., FindShortestTour function is used for ordering boundary points. These data are passed on collectively as input to further functions to compute the shape and size of particles. Additionally, two geometric features – diameter of inscribed circle and circumscribed circle - are computed for calculation of textural parameters (listed in section 2.3). They are only stored internally and are fed into functions that require them. The radius and the centre of the largest inscribed circle of each particle is computed by the function **InscribedCircle**. Here the minimum distance from any point inside the particle boundary to the particle boundary is maximised using discrete optimisation with multiple starting points. Similarly, **CircumscribedCircle** function computes the smallest circumscribing circle over the particle boundary by minimising the maximum distance from any point inside the particle boundary to the particle boundary.

2.3. Computation of textural parameters

Measurements in this paper are focused on a 2-dimensional representation of the particle boundary. In case of loose sediments, projection of particles along the long and intermediate axis is taken, whereas, a 2D section of sediments cutting across consolidated sample is available from a thin section. A large number of parameters have been proposed to quantify particle shape (Barrett, 1980; Blott and Pye, 2008 and references therein). It is difficult to select one parameter out of the many available, that allows for consistent, reliable and accurate distinction between particles of different shapes. As a result, the relative merits of different shape parameters have been extensively reviewed along with the many practical studies making comparisons (Al-Rousan et al., 2007; Barrett, 1980; Blott and Pye, 2008; Cox and Budhu, 2008; Illenberger, 1991). In light of their application to 2-D image data, the following parameters are discussed and implemented: roundness, circularity, irregularity, angularity, fractal dimension, Fourier descriptors and a number of other simpler dimensionless parameters such as aspect ratio, rectangularity, convexity, modratio, compactness and solidity. Additionally, a variety of size parameters are implemented. The implementation details and description of parameters are described below:

2.3.1. Roundness

The most widely accepted definition of roundness (Wadell, 1932) is that it is the average roundness of the corners of a particle in a 2-D sectional plane. Let r be the radius of curvature of the boundary and let r_{max} be the radius of the largest inscribed circle to the particle boundary. Corners are those parts of the particle boundary where $r < r_{max}$. Particle roundness (R) is defined as:

$$R = \frac{1}{n\, r_{max}} \sum_{i=1}^{n} r_i$$

where r_i is the radius of curvature of individual corner and n is the total number of corners. Roundness can now be determined in a time efficient and objective manner using computational image analysis techniques (Roussillon et al., 2009; Tunwal et al., 2018).

The **Roundness** function first calculates the radius of curvature at each point on the boundary. It makes use of the function **CircumRadius,** which determines the radius of the circle circumscribing three points: 1) *i*th pixel at which radius of curvature is to be determined, 2) *(i+n)*th pixel and 3) *(i-n)*th pixel (see Fig. 4a). The value of *n* is normalised on the basis of total number of boundary points in the particle. In Figure 4, point A, B and C represents the $(i-n)$th, ith and $(i+n)$th pixel respectively. Points with a radius of curvature greater than radius of the largest inscribed circle of the particle (from InscribedCircle function) are omitted (see Fig. 4b). The mean of the radius of curvature of the remaining points divided by radius of the largest inscribed circle is the roundness.

2.3.2. Circularity

Circularity is a measure of how closely a particle boundary approximates to a circle. Typical circularity parameters (Cox, 1927; Janoo, 1998; Pentland, 1927; Riley, 1941; Wadell, 1933; Wadell, 1935) were applied to 23 gravel particles in a comparison study (Blott and Pye, 2008). They found that the methods of Wadell (1935) and Riley (1941) provided optimal results. Due to its simplicity and similarity to Wadell (1935), Riley (1941) was considered to be the best parameter and is implemented in IPSAT. It is given by:

$$C = \sqrt{(D_I/D_c)}$$

where C is the circularity, D_I is the diameter of largest inscribed circle and D_c is the diameter of smallest circumscribing circle (see Fig. 5). The **CircularityFunction** takes radius of the largest inscribed circle of the particle from InscribedCircle and the radius of the smallest circumscribing circle of the particle from CircumscribedCircle to compute circularity.

2.3.3. Irregularity

Irregularity has been recently suggested as a parameter to describe particle shape (Blott and Pye, 2008). It is defined as a way to measure the indentations and projections of a particle boundary with respect to the best fit ellipse (Tunwal et al., 2018). It is given by:

$$\mathrm{I} = \mathrm{A_U}/\mathrm{A_E}$$

Where I is the irregularity, A_U is the non-overlapping area and A_E is the area of ellipse (see Fig. 6). The value for irregularity varies in the range 0 to 1. Particle with smooth boundary exhibits lower value for irregularity as compared to a particle with irregular boundary. The **Irregularity** function generates two matrices for each particle: the first represents points belonging to the particle and the second consists of points inside the best-fit ellipse of the particle. Thus, addition of the matrices identifies the non-overlapping region used for calculating irregularity.

2.3.4. Angularity

Angularity is usually considered the opposite of roundness, however it is formally defined as a shape parameter based on acuteness of angle of corners, number of corners and projection of corners from the centre of particle (Lees, 1964). To measure angularity, the **Angularity** function converts the particle boundary into a n sided polygon by sampling n points at regular interval along the particle boundary points (Rao et al., 2002). The internal angle at each vertex is

computed, which is represented by α_1 to α_n. The difference between the pair of consecutive angles (α_1-α_2, α_2-α_3 to α_n-α_1) of the polygon is calculated for all vertices (see Fig. 7). The average of the five largest differences of angles is the angularity (Tunwal et al., 2018). The number of sides of regular polygon that represents the particle boundary and the number of highest differences of consecutive angles can be varied by user.

2.3.5. Fractal dimension

Benoit Mandelbrot is credited with discovering the field of Fractal geometry in mathematics to characterise irregular shapes and quantify their roughness (Mandelbrot, 1982). Using fractal dimension as a measure of roughness in granular materials is already established (Andrle, 1992; Cox and Budhu, 2008; Hyslip and Vallejo, 1997; Tunwal et al., 2018).

The **FractalDivider** function is implemented in IPSAT using the divider method. This method essentially measures the length of the boundary using different measuring sticks and uses the relationship between the two to estimate the fractal dimension (see Fig. 8a). If the length of the boundary of a shape is measured to be $P(\lambda)$, using measure of length λ then

$$P(\lambda) = n\lambda^{1-D}$$

where D is the fractal dimension and n is a constant of proportionality, which depends on the actual length of the boundary being analysed. Lower values of λ result in more accurate and increased estimates of boundary length $P(\lambda)$. Taking logarithms:

$$\log P(\lambda) = \log n + (1 - D) \log \lambda$$

thus D may be readily estimated by finding the best fit straight line to a set of data of $(\log \lambda, \log P(\lambda))$ (see Fig. 8b). The unit divider length λ in IPSAT depend on the size of each individual particle (normalised based on the axes of the best fit ellipse).

2.3.6. Fourier method

Half a century ago, Fourier analysis was introduced as an accurate way to characterise sediment particle shape (Schwarcz and Shane, 1969; Ehrlich and Weinberg, 1970). Fourier analysis is based on the fact that any periodic function can be represented by a series of sine and cosine terms. Fourier analysis is applied in shape characterisation by unrolling the particle boundary and treating it as a periodic wave function and using the centroid of the particle as the origin. The particle boundary can be reconstructed to a high degree of accuracy by using a suitable number of terms. In spite of being robust, Fourier analysis in this context is not ideal due to the re-entrant angle problem. Re-entrants are due to jagged or crenellate edge morphology in irregular shaped particles (Orford and Whalley, 1983) and leads to re-entrant angle or multi-valued function problem (Bowman et al., 2001; Thomas et al., 1995). To overcome the shortcoming of re-entrant angle, Fourier descriptors are used (Thomas et al., 1995).

In this technique, the particle boundary is first sampled at regular intervals. Each boundary point is represented in the complex plane by:

$$z_m = x_m + \boldsymbol{i}\, y_m$$

where (x_m, y_m) are the coordinates, m goes from 0 to $(N-1)$ and N is the total number of sampled points. The discrete Fourier transform is applied to the list of boundary points to obtain the list of descriptors as follows:

$$\mathrm{Z_k} = \frac{1}{\mathrm{N}} \sum_{m=0}^{N-1} z_m e^{-i\frac{2\pi mk}{N}} = \frac{1}{N} \sum_{m=0}^{N-1} z_m (\cos \frac{2\pi mk}{N} - \boldsymbol{i} \sin \frac{2\pi mk}{N})$$

The Fourier descriptors are $Z_k = a_k + ib_k$ where k takes the values 0 to $N-1$.

Applying the inverse Fourier transform to the descriptors retrieves estimates of the boundary points of a particle and thus can be used to reconstruct the original shape of the particle. Often only a subset of the full set of Fourier descriptors are utilised for a particle. As the number of Fourier descriptors used to describe a shape increases, the boundary retrieved by the inverse transform becomes more accurate (see Fig. 9). Descriptors with low values of k tend to describe the major features of a particle whereas those with high values of k describe the finer morphological details.

Fourier descriptors are computed using the **FourierDescriptor** function. In this function, the boundary is sampled at regular interval to take a total of n points for each particle, where n can be set by user. The centre of the particle boundary is shifted to the origin to compute the n number of Fourier descriptors. The output to a file type of user's choice can be exported using **FourierOutput** function.

2.3.7. Other parameters

Shape parameters, which were traditionally not taken into account from a sedimentological point of view but can prove useful in discriminating different types of sedimentary particles, are also included in IPSAT. Cox and Budhu (2008) studied many simple parameters and identified key parameters to discriminate amongst sedimentary particles (see Table 1). These parameters are calculated directly using basic geometric features extracted earlier (see section 2.2). They can be viewed and exported along with other results using ResultTable function described in section 2.4.

2.3.8 Particle Size

In this paper, the size of sand particles is measured using image analysis techniques on a microphotograph. However, the methodology presented here can be extended to images of particles from other size fractions. **SizeData** function is written to compute the actual size of particle regions by parameters listed in Table 2. The user is required to specify the actual width of the input image so that IPSAT can convert pixel units to standard physical units (i.e. microns or millimetres). Thus it has three arguments: the output from GrabImage, CircumscribedCircle and the actual width.

Due to slicing of grains in thin section, the measured size of a particle from a thin section microphotograph is usually less than the size measured from the projection on a loose grain (Burger and Skala, 1976). There are multiple approaches in the field stereology to transform a 2-D particle size distribution to a 3-D size distribution (Mouton, 2011; Russ and Dehoff, 2000). Some authors have recommended using a simple multiplication factor for the size transformation (for example, Harrell and Eriksson, 1979; Kong et al., 2005), however, others have recommended using a size distribution transformation algorithm (Heilbronner and Barrett, 2014;

290 Higgins, 2000; Peterson, 1996). In this paper, one such , which assumes that the probability of
291 slicing a particle is dependent on its size and distance from centre is implemented (Heilbronner
292 and Barrett, 2014; Underwood, 1970).

293 The **SizeTransform** function is available to convert a 2-D size distribution to a 3-D size
294 distribution. This function takes data from **SizeData** as input along with class distribution width
295 and the numeral code for the type of size parameter to be used. The algorithm implemented in
296 IPSAT follows the method described in Heilbronner and Barrett (2014) for STRIPSTAR
297 program.

298 2.4. Results

299 Results obtained for all particles in a sample can be summarised in tabular form and exported to
300 an excel file. Users can specify the parameters they wish to include in the output. The function
301 **ResultTable[***exdata_*, *parameters_*,*others_*,*sizedata_***]** is written for this purpose. The argument
302 *parameters_* specifies the list of parameters that are required by the user. This provides
303 flexibility and saves execution time. The third argument *others_* may be either *True* or *False* and
304 indicates whether or not to include in the output the other parameters in the result table. The
305 fourth argument *sizedata* _ takes in the output from **SizeData**, if size is required. These other
306 parameters include simple geometric data such as aspect ratio, rectangularity, convexity,
307 modratio, compactness and solidity (see Table 1).

308 Finally, a data visualisation function called **GrainMapping** is present to display regions of
309 particle using varying colour scheme based on output of a chosen shape or size parameter (see
310 Fig. 10). This feature has been used in other image analysis tools (e.g. Heilbronner and Barrett,
311 2014) and is presented here for completeness.

3. Example Analysis

One sample each of unconsolidated (loose sediment) and consolidated (rock thin section) is analysed to demonstrate the usage of this software package. A total of 60 particles were analysed for both examples. Details of the samples and their image preparation methodology are discussed below.

3.1. Loose sediment

A loose sediment sample from Ballycotton beach, County Cork, Ireland was collected for particle shape analysis. The sample is dry sieved to separate the different size fractions. For example analysis, the 250 to 500 Microns size fraction is used. The sand grains are carefully settled on the microscope stage parallel to their longest and intermediate axis. Using a paint brush, these particles are set up such that they do not touch each other and remain within the field of view of the microscope. For each field of view, 5-7 particles were imaged (see Fig. 2a). The images were captured at 140X for 1640*2186 microns field of view at 1200*1600 Pixel resolution. The following settings were used for the microscope for transmitted light from beneath the stage: exposure 61.4 ms; saturation: 1.3; gain: 1.0X; gamma 1.29.

3.2. Rock thin section

A sandstone sample from Dingle Basin, South-West Ireland was collected for thin section analysis. The sample collected is from the Eask Sandstone Formation of the Dingle group and is relatively undeformed. The sediment particles in the sample were deposited in a fluvial type of depositional environment during the Lower Devonian (Allen and Crowley, 1983). The sample shows poorly sorted quartz grains surrounded by a clay matrix (Fig. 3a).

Thin section images of each sample in cross-polarised light were used for tracing out particle boundaries. Using more than one image of the same field of view at different stage orientations in cross-polarised light may increase clarity for tracing particle boundaries. An Intuos Pro Graphics Tablet was used to digitally trace the boundaries in CorelDRAW, which is a vector graphics editing software. Digital tracing of particle boundaries allows the flexibility of zooming in and out on the field of view and browse through microphotographs at different stage orientations while tracing. Each particle boundary is traced carefully so that they form a closed loop otherwise they are not detected as a separate region during the image processing step. It is important to ensure that the particle boundaries do not touch each other (Fig. 3b). The particle boundaries can be alternately traced physically on a tracing sheet and digitised for analysis (refer to Mulchrone et al. (2013) for details). The traced image is 1.86 Mb in size (1600*1200 pixels). The physical size of the thin section image is 1640*2186 Microns determined using Leica Microscope software.

4. Results and Discussion

The result of particle shape analysis for the loose sediment sample is presented in the form of histogram (Fig. 11). Roundness, angularity, irregularity and fractal dimension data display a normal distribution. Circularity data for the population show a negative skew, whereas, there is positive skewness in the aspect ratio data distribution. The mean and standard deviation of: roundness is 0.61 and 0.04; angularity is 54.04 and 10.93; irregularity is 0.14 and 0.05; and fractal dimension is 1.02 and 0.01 respectively. The median of circularity and aspect ratio data is 0.82 and 1.32 respectively.

Figure 12 shows the population distribution of shape parameters from the sandstone thin section sample. The datasets of roundness, circularity, irregularity and angularity exhibit normal

distributions, whereas, fractal dimension and aspect ratio show positively skewed distributions. The mean and standard deviation of: roundness is 0.60 and 0.04; circularity is 0.76 and 0.06; irregularity is 0.17 and 0.05; and angularity is 53.92 and 10.94. The median of fractal dimension and aspect ratio is 1.03 and 1.51 respectively.

The image analysis package –IPSAT presented in this paper can be used to measure a range of shape and size parameters. More than one shape parameter can be used to better characterise a particle shape (Blott and Pye, 2008). The shape parameters implemented here were tested on regular geometric shapes (Blott and Pye, 2008) and were found to perform well. A previous study by the authors (Tunwal et al., 2018) found angularity and fractal dimension to be the most important parameters for classifying sediment samples in their textural maturity grouping. However, presence of a comprehensive list of shape parameters in IPSAT offers a choice to users from diverse research objectives. It is to be noted that the term angularity, roundness and circularity are defined differently in various software tools. For e.g., roundness in ImageJ (Schneider et al., 2012) refers to the ratio $4Area/\pi(MajorAxis)^2$, whereas, roundness in IPSAT is based on calculation of radius of curvature at each boundary point (Roussillon et al., 2009). Fourier descriptors, function available in IPSAT, exports fourier descriptor data in raw form. This is to facilitate users the flexibility to choose their preferred way of further analysis (for e.g., Bowman et al., 2001; Charpentier et al., 2013; Suzuki et al., 2015; Thomas et al., 1995; Haines and Mazzullo, 1988; Sarocchi et al., 2011).

IPSAT offers a variety of size parameters for analysis. Different measures of size give different particle size distributions for the same population of particles (Heilbronner and Barrett, 2014). Therefore, a suite of size parameters implemented here gives the user the freedom to pick the parameters of choice. For thin section images, 2-Dimensional particle size distribution should be

transformed into 3-Dimensional size distribution for analysis. Apart from the shape and size parameters presented in IPSAT, some additional information regarding the particles can be further obtained implicitly from the results. For example, area and perimeter of particles can be calculated from the size measures S_d and S_p. Such information can be extracted, if required, by the user.

The manual particle boundary tracing for thin section analysis can be regarded by some as a tedious exercise. However, in the light of unavailability of an automated particle boundary segmentation algorithm that can be used for any type of thin section image, manual particle boundary tracing provides the best alternative at present. High quality shape and size information can be easily obtained once the boundary is traced. Furthermore, the whole methodology is relatively cheap to perform. If new analysis techniques emerge which can process messy natural data, the analysis software presented here will be fully compatible and the process can be fully automated.

The shape parameters calculated using particle boundary data in this package is independent of size. However, a particle of a very small pixel size is prone to be affected by its size for shape calculation (Kröner and Doménech Carbó, 2013). Regular geometric and irregular shape with increasing pixel count were used to test this package to check variation of parameter values with varying pixel count for a fixed shape. It was found it is not affected by size (S_c) above 85 pixels. Thus, size limit for textural analysis of sediment is based on the image acquisition tool. Furthermore, a higher pixel resolution is recommended for good results.

The contribution presented here will help in filling the gap for a specialised texture analysis toolbox in the domain of sedimentology. The use of the software package introduced here has been demonstrated by examples with sand sized particles. However, it can be used for particles

of any size. Therefore, the image analysis package can be of use to variety of users for diverse shape analysis objectives.

5. Conclusion

In this paper, IPSAT – Image based Particle Shape Analysis Toolbox is presented for determination of textural elements of sedimentary particles. A suite of 12 shape parameters and 6 size parameters are implemented in IPSAT. Usage of the presented toolbox has been demonstrated using photomicrographs from a sandstone thin section and a loose sediment sample. Manual tracing of particles of thin section particle boundaries is recommended, whereas, a fully automated approach is available for loose sediment analysis.

The software along with the methodology proposed in this paper, has the potential for allowing access to quantitative data for textural elements of siliciclastic particles. Thus, it has the potential to provide important information for a wide range of sedimentary studies. Future work in the direction of quantitative textural analysis of sedimentary particles include development of a statistical approach aimed at synthesis and analysis of distributions of sediment particle shape population data.

6. Acknowledgement

The authors are thankful to the Chief Editor and the three anonymous reviewers for their suggestions which has substantially improved the manuscript. This project was funded by the Irish Shelf Petroleum Studies Group (ISPSG) of the Irish Petroleum Infrastructure Programme (PIP).

7. Computer Code Availability

The Image based Particle Shape Analysis Toolbox (IPSAT) is developed as a Mathematica package (26 Kb). The IPSAT code is written on Wolfram language which requires Mathematica environment to function. The IPSAT package is released under the GPL3 license. The IPSAT code along with a detailed user manual can be downloaded from https://github.com/tunwalm/IPSAT. The developer can be contacted reached by the following:

Email: mohit.tunwal@ucc.ie

Telephone: +353-21-490-4580

Address: School of BEES, University College Cork, Distillery Fields, North Mall, Cork, T23 TK30, Ireland

8. References

Al-Rousan, T., Masad, E., Tutumluer, E. and Pan, T. (2007) Evaluation of image analysis techniques for quantifying aggregate shape characteristics. *Construction and Building Materials*, **21,** 978-990.

Allen, J.R.L. and Crowley, S.F. (1983) Lower Old Red Sandstone fluvial dispersal systems in the British Isles. Transactions of the Royal Society of Edinburgh: Earth Sciences, **74,** 61-68.

Andrle, R. (1992) Estimating fractal dimension with the divider method in geomorphology. *Geomorphology*, **5,** 131-141.

Barrett, P.J. (1980) The shape of rock particles, a critical review. Sedimentology, **27,** 291-303.

Blatt, H. (1992) Sedimentary Petrology. W. H. Freeman and Company, New York, 514 pp.

Blatt, H., Middleton, G. and Murray, R. (1972) Origin of Sedimentary Rocks. Prentice-Hall Inc., Upper Saddle, NJ, 634 pp.

Blott, S.J. and Pye, K. (2008) Particle shape: a review and new methods of characterization and classification. Sedimentology, **55,** 31-63.

Bowman, E.T., Soga, K. and Drummond, W. (2001) Particle shape characterisation using Fourier descriptor analysis. Géotechnique, **51,** 545-554.

Burger, H. and Skala, W. (1976) Comparison of sieve and thin-section technique by a Monte-Carlo model. Computers & Geosciences, **2,** 123-139.

Calderon De Anda, J., Wang, X.Z. and Roberts, K.J. (2005) Multi-scale segmentation image analysis for the in-process monitoring of particle shape with batch crystallisers. *Chemical Engineering Science*, **60,** 1053-1065.

Campaña, I., Benito-Calvo, A., Pérez-González, A., Bermúdez de Castro, J.M. and Carbonell, E. (2016) Assessing automated image analysis of sand grain shape to identify sedimentary facies, Gran Dolina archaeological site (Burgos, Spain). Sedimentary Geology, **346,** 72-83.

Charpentier, I., Sarocchi, D. and Rodriguez Sedano, L.A. (2013) Particle shape analysis of volcanic clast samples with the Matlab tool MORPHEO. Computers & Geosciences, **51,** 172-181.

Cox, E.P. (1927) A Method of Assigning Numerical and Percentage Values to the Degree of Roundness of Sand Grains. Journal of Paleontology, **1,** 179-183.

Cox, M.R. and Budhu, M. (2008) A practical approach to grain shape quantification. Engineering Geology, **96,** 1-16.

Eamer, J.B.R., Shugar, D.H., Walker, I.J., Lian, O.B. and Neudorf, C.M. (2017) Distinguishing depositional setting for sandy deposits in coastal landscapes using grain shape. Journal of Sedimentary Research, **87,** 1-11.

Ehrlich, R. and Weinberg, B. (1970) An exact method for characterization of grain shape. Journal of Sedimentary Research, **40**, 205-212.

Gorsevski, P.V., Onasch, C.M., Farver, J.R. and Ye, X. (2012) Detecting grain boundaries in deformed rocks using a cellular automata approach. Computers & Geosciences, **42,** 136-142.

Haines, J. and Mazzullo, J. (1988) The original shapes of quartz silt grains: A test of the validity of the use of quartz grain shape analysis to determine the sources of terrigenous silt in marine sedimentary deposits. *Marine Geology*, **78**, 227-240.

Harrell, J.A. and Eriksson, K.A. (1979) Empirical conversion equations for thin-section and sieve derived size distribution parameters. Journal of Sedimentary Research, **49,** 273-280.

Heilbronner, R. and Barrett, S. (2014) Image analysis in earth sciences: microstructures and textures of earth materials. Springer, Heidelberg, 513 pp.

Higgins, M.D. (2000) Measurement of crystal size distributions. American Mineralogist, **85,** 1105-1116.

Higgins, M.D. (2006) Quantitative textural measurements in igneous and metamorphic petrology. Cambridge University Press, Cambridge, 265 pp.

Hyslip, J.P. and Vallejo, L.E. (1997) Fractal analysis of the roughness and size distribution of granular materials. Engineering Geology, **48,** 231-244.

Illenberger, W.K. (1991) Pebble shape (and size!). Journal of Sedimentary Research, **61,** 756-767.

Janoo, V. 1998. Quantification of shape, angularity, and surface texture of base course materials, Cold Regions Research and Engineering Lab Hanover NH.

Kong, M., Bhattacharya, R.N., James, C. and Basu, A. (2005) A statistical approach to estimate the 3D size distribution of spheres from 2D size distributions. GSA Bulletin, **117,** 244-249.

Kröner, S. and Doménech Carbó, M.T. (2013) Determination of minimum pixel resolution for shape analysis: Proposal of a new data validation method for computerized images. Powder Technology, **245,** 297-313.

Krumbein, W.C. (1941) Measurement and geological significance of shape and roundness of sedimentary particles. Journal of Sedimentary Research, **11**, 64-72.

Lees, G. (1964) A NEW METHOD FOR DETERMINING THE ANGULARITY OF PARTICLES. Sedimentology, **3,** 2-21.

Li, Y., Onasch, C.M. and Guo, Y. (2008) GIS-based detection of grain boundaries. Journal of Structural Geology, **30,** 431-443.

Lira, C. and Pina, P. (2009) Automated grain shape measurments applied to beach sands. Journal of Coastal Research**,** 1527-1531.

Mandelbrot, B.B. (1982) The Fractal Geometry of Nature. W. H. Freeman and Company, New York, NY, 468 pp.

Mingireanov Filho, I., Vallin Spina, T., Xavier Falcão, A. and Campane Vidal, A. (2013) Segmentation of sandstone thin section images with separation of touching grains using optimum path forest operators. Computers & Geosciences, **57,** 146-157.

Moreno Chávez, G., Castillo Rivera, F., Sarocchi, D., Borselli, L. and Rodríguez-Sedano, L. (2018) FabricS: A user-friendly, complete and robust software for particle shape-fabric analysis. Computers & Geosciences, **115,** 20-30.

Moreno Chávez, G., Sarocchi, D., Arce Santana, E. and Borselli, L. (2015) Optical granulometric analysis of sedimentary deposits by color segmentation-based software: OPTGRAN-CS. *Computers & Geosciences*, **85,** 248-257.

Mouton, P.R. (2011) *Unbiased stereology: a concise guide*. JHU Press, Baltimore, Maryland, 200 pp.

Mulchrone, K.F., McCarthy, D.J. and Meere, P.A. (2013) Mathematica code for image analysis, semi-automatic parameter extraction and strain analysis. Computers & Geosciences, **61,** 64-70.

Orford, J.D. and Whalley, W.B. (1983) The use of the fractal dimension to quantify the morphology of irregular-shaped particles. Sedimentology, **30,** 655-668.

Pentland, A. (1927) A method of measuring the angularity of sands. Proceedings and Transactions of the Royal Society of Canada, **21,** xciii.

Peterson, T.D. (1996) A refined technique for measuring crystal size distributions in thin section. Contributions to Mineralogy and Petrology, **124,** 395-405.

Pettijohn, F.J. (1957) Sedimentary Rocks. Harper & Brothers, New York, 718 pp.

Powers, M.C. (1953) A new roundness scale for sedimentary particles. Journal of Sedimentary Research, **23**, 117-119.

Rao, C., Tutumluer, E. and Kim, I.T. (2002) Quantification of Coarse Aggregate Angularity Based on Image Analysis. Transportation Research Record: Journal of the Transportation Research Board, **1787,** 117-124.

Riley, N.A. (1941) Projection sphericity. Journal of Sedimentary Research, **11**, 94-97.

Roduit, N. (2007) JMicroVision: un logiciel d'analyse d'images pétrographiques polyvalent. Ph.D. Dissertation, University of Geneva, Geneva, Switzerland, 112pp.

Roussillon, T., Piégay, H., Sivignon, I., Tougne, L. and Lavigne, F. (2009) Automatic computation of pebble roundness using digital imagery and discrete geometry. Computers & Geosciences, **35,** 1992-2000.

Roy Choudhury, K., Meere, P.A. and Mulchrone, K.F. (2006) Automated grain boundary detection by CASRG. Journal of Structural Geology, **28,** 363-375.

Russ, J.C. and Dehoff, R.T. (2000) *Practical stereology*. Plenum Publishers, New York, 381 pp.

Sarocchi, D., Sulpizio, R., Macías, J.L. and Saucedo, R. (2011) The 17 July 1999 block-and-ash flow (BAF) at Colima Volcano: New insights on volcanic granular flows from textural analysis. *Journal of Volcanology and Geothermal Research*, **204**, 40-56.

Schneider, C.A., Rasband, W.S. and Eliceiri, K.W. (2012) NIH Image to ImageJ: 25 years of image analysis. Nature Methods, **9,** 671-675.

SCHWARCZ, H.P. and SHANE, K.C. (1969) MEASUREMENT OF PARTICLE SHAPE BY FOURIER ANALYSIS. *Sedimentology*, **13**, 213-231.

Sochan, A., Zieliński, P. and Bieganowski, A. (2015) Selection of shape parameters that differentiate sand grains, based on the automatic analysis of two-dimensional images. Sedimentary Geology, **327,** 14-20.

Suzuki, K., Fujiwara, H. and Ohta, T. (2015) The evaluation of macroscopic and microscopic textures of sand grains using elliptic Fourier and principal component analysis: Implications for the discrimination of sedimentary environments. Sedimentology, **62,** 1184-1197.

Takashimizu, Y. and Iiyoshi, M. (2016) New parameter of roundness R: circularity corrected by aspect ratio. Progress in Earth and Planetary Science, **3,** 1-16.

Tao, J., Zhang, C., Qu, J., Yu, S. and Zhu, R. (2018) A de-flat roundness method for particle shape quantitative characterization. Arabian Journal of Geosciences, **11,** 414.

Thomas, M.C., Wiltshire, R.J. and Williams, A.T. (1995) The use of Fourier descriptors in the classification of particle shape. Sedimentology, **42,** 635-645.

Trott, M. (2013) *The Mathematica guidebook for programming*. Springer, New York, 1027 pp.

Tunwal, M., Mulchrone, K.F. and Meere, P.A. (2018) Quantitative characterization of grain shape: Implications for textural maturity analysis and discrimination between depositional environments. Sedimentology, **65,** 1761-1776.

Underwood, E.E. (1970) Quantitative Stereology. Addison-Wesley Pub. Co., Reading, Mass., 274 pp.

Wadell, H. (1932) Volume, Shape, and Roundness of Rock Particles. The Journal of Geology, **40,** 443-451.

Wadell, H. (1933) Sphericity and roundness of rock particles. The Journal of Geology, **41,** 310-331.

Wadell, H. (1935) Volume, Shape, and Roundness of Quartz Particles. The Journal of Geology, **43,** 250-280.

Wellin, P.R., Gaylord, R.J. and Kamin, S.N. (2005) *An introduction to programming with Mathematica®*. Cambridge University Press, Cambridge, UK, 570 pp.

Figure Captions

Figure 1: Flowchart showing functionality of IPSAT program.

Figure 2: Image analysis routine for loose sediment analysis. (a) Shows microphotograph of loose sand sample collected from Ballycotton, County Cork, Ireland. (b) Particle boundary of the sediment grains from the loose sediment sample is automatically generated using IPSAT (c) image analysis of particle boundary shows region in randomly assigned colours identified as individual particles.

Figure 3: Image analysis routine for a compacted sample (a) Shows thin section microphotograph of sandstone sample collected from Dingle, County Kerry, Ireland. (b) Particle

582 *boundary of the clasts from thin section is manually traced using a graphics tablet (c) image*
583 *analysis of traced particle boundary shows region in randomly assigned colours identified as*
584 *individual particles.*

585 *Figure 4: Roundness measurement of a particle boundary. (a) Calculation of radius of curvature*
586 *at the ith pixel point B is the radius of circle that passes through the points A,B and C. The*
587 *points A and C are the $(i+n)^{th}$pixel and $(i-n)^{th}$pixel where n is normalised on the basis*
588 *total number of boundary points. (b) The particle boundary points with radius of curvature lower*
589 *than the radius of largest inscribing circle represents the corner region and are thus accepted*
590 *for roundness calculation.*

591 *Figure 5: Circularity of particle measured by square root over the ratio of diameter of the*
592 *largest inscribed circle (D_i) divided by the diameter of the smallest circumscribed circle (D_c).*

593 *Figure 6: Measurement of particle irregularity. (a) Particle boundary to be analysed. (b) Best fit*
594 *ellipse for the particle boundary to be analysed. (c) Overlap of best fit ellipse over the particle*
595 *boundary. Irregularity is measured as a ratio of area not common between ellipse and particle*
596 *boundary divided by the area of ellipse.*

597 *Figure 7: Angularity measurement of a particle by modified Rao et al. (2002). Particle boundary*
598 *is represented by n sided polygon. Internal angles α_1, α_2, α_3 till α_n for the polygon is measured.*
599 *Differences within the successive internal angles is measured and the five largest differences of*
600 *internal angles are averaged to calculate angularity.*

601 *Figure 8: Fractal dimension calculation for a particle using the divider method. (a) Particle*
602 *boundary perimeter $P(\lambda)$ measured by increasing unit length λ. The value of m is 13.28 pixel*

603 *dimension based on the size of the particle. (b) Log $P(\lambda)$ versus Log λ showing the fractal*
604 *dimesion (D) calculation.*

605 *Figure 9: Reconstructed particle boundary with the number of Fourier descriptors used from*
606 *k=1 to 15. Shows the increasing accuracy of the particle boundary with the number of*
607 *descriptors used.*

608 *Figure 10: Grain-map of thin section sample for angularity parameter. The colour varies from*
609 *light green for highest roundness to dark blue for highest angularity value.*

610 *Figure 11: Results from photomicrograph analysis of loose sediment sample represented by*
611 *histogram for: (a) roundness; (b) circularity; (c) irregularity; (d) angularity; (e) fractal*
612 *dimension; and (f) aspect ratio data*

613 *Figure 12: Results from thin section photomicrograph analysis of sandstone sample represented*
614 *by histogram for: (a)roundness; (b) circularity; (c) irregularity; (d) angularity; (e) fractal*
615 *dimension; and (f) aspect ratio data*

616

617 # Tables

618

619

620

Shape Parameter	Formula	Description
Aspect Ratio	L_{major}/L_{minor}	Length of major axis (L_{major}) by length of minor axis

		(L_{minor})
Compactness	$\sqrt{4A/\pi}$/L_{major}	Diameter of circle of equivalent area (A) to particle by length of major axis (L_{major})
ModRatio	$2R_I$/Feret	Diameter of largest inscribed circle (R_I) divided by Feret diameter
Solidity	A/A_{convex}	Area (A) by convex area (A_{convex})
Convexity	P_{convex}/P	Convex perimeter (P_{convex}) by perimeter of particle (P)
Rectangularity	A/A_{BR}	Area of particle (A) by area of bounding rectangle (A_{BR})

Table 1: Table of simple geometrical parameters used in the study.

Size parameter	**Formula**	**Description**
S_c	D_c	Diameter of smallest circumscribing circle over a particle boundary

S_p	P/π	Perimeter of particle boundary (P) divided by π
S_d	$\sqrt{4A/\pi}$	Diameter of equivalent disk area of the particle. Here A is the area of the particle.
S_a	L_{major}	Long axis of the best fit ellipse (L_{major})
S_b	L_{minor}	Short axis of the best fit ellipse (L_{minor})
S_m	$\frac{2\sum_{i=1}^{n}(d_i)}{n}$	Twice of the mean distance between centre and particle boundary. Here d_i is the distance between centroid of the particle to its ith boundary point and n is the number of boundary points.

629

630 *Table 2: List of size parameters implemented in IPSAT.*

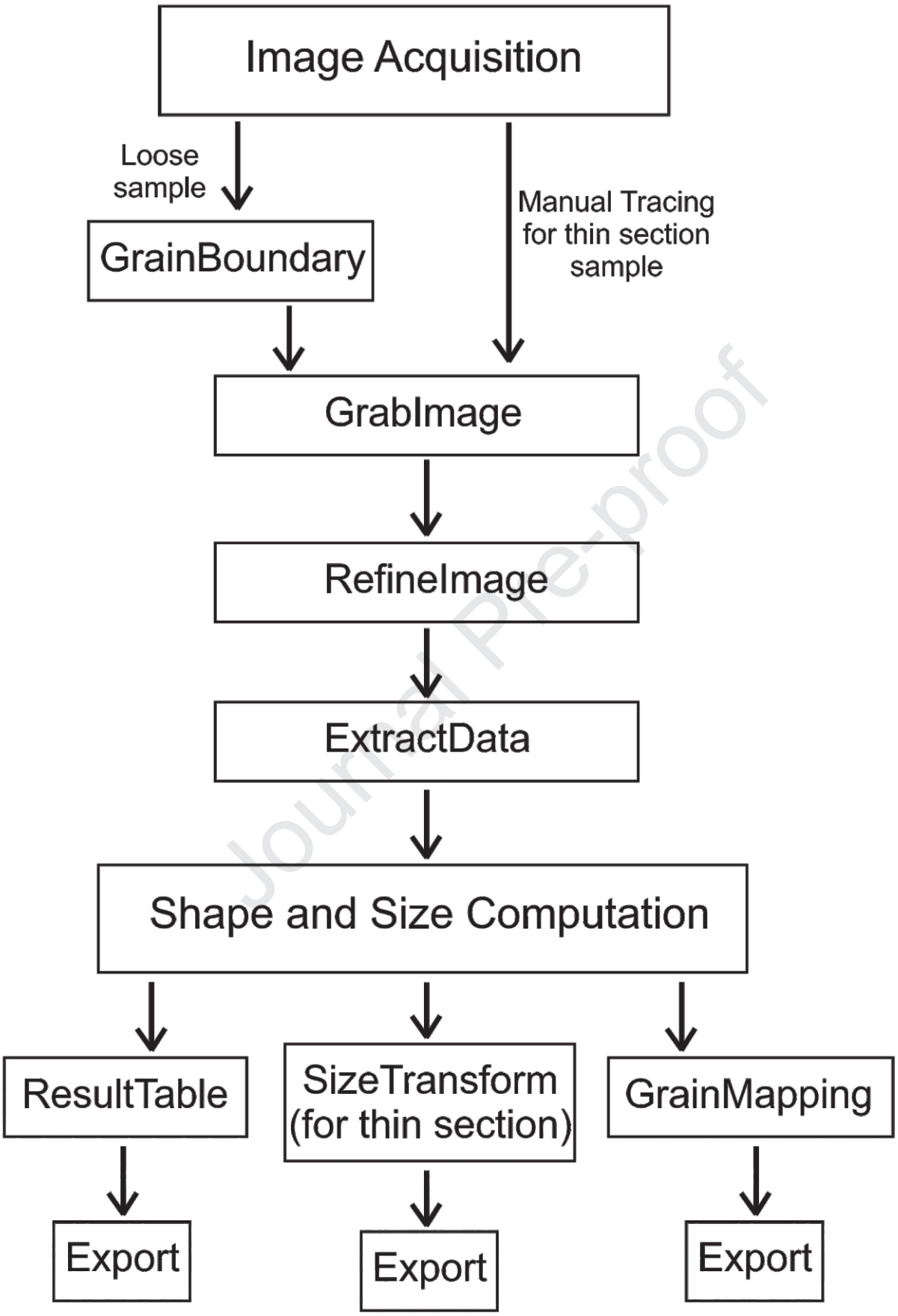
Image Acquisition
Loose sample
Manual Tracing for thin section sample
GrainBoundary
GrabImage
RefineImage
ExtractData
Shape and Size Computation
ResultTable
SizeTransform (for thin section)
GrainMapping
Export
Export
Export

Figure 1

(A)

(B)

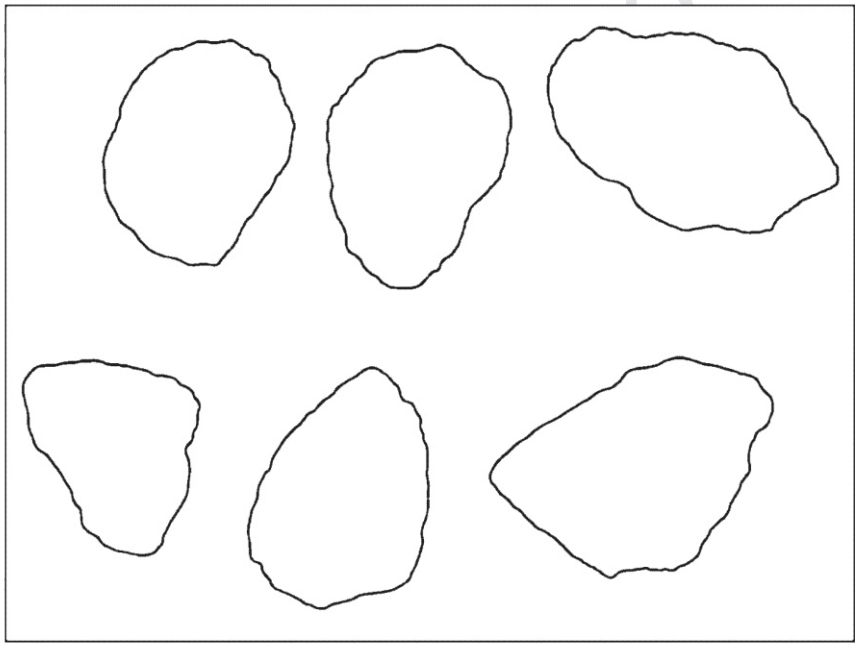

(C)

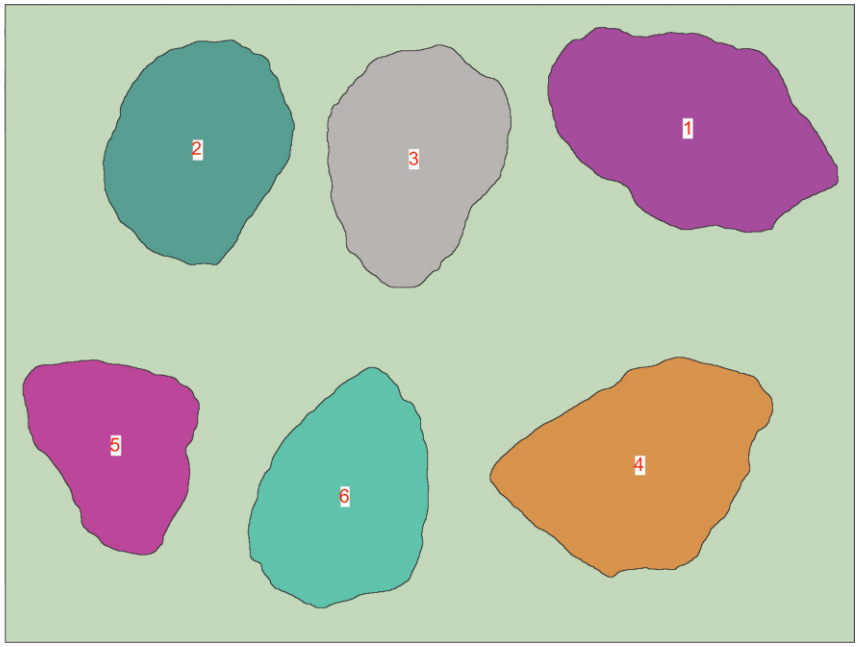

Figure 2

(A)

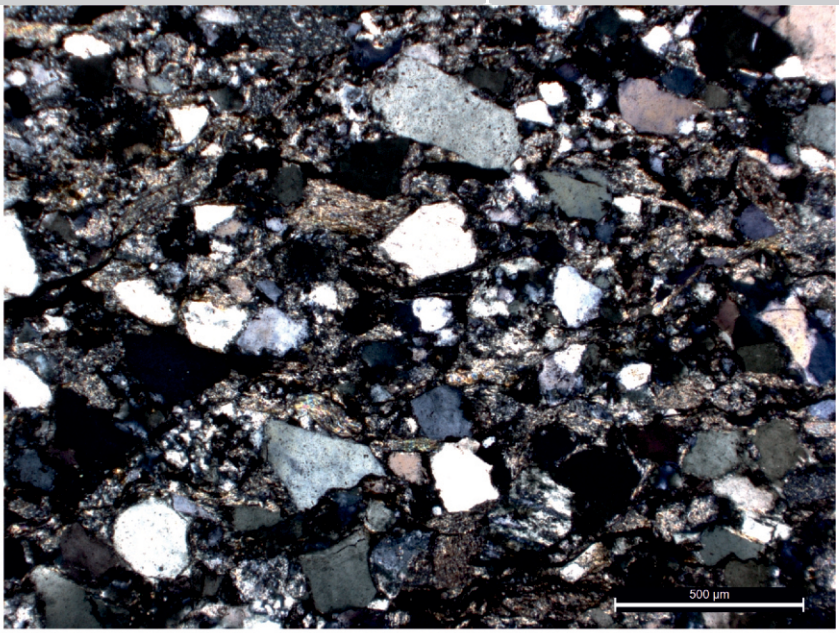

(B)

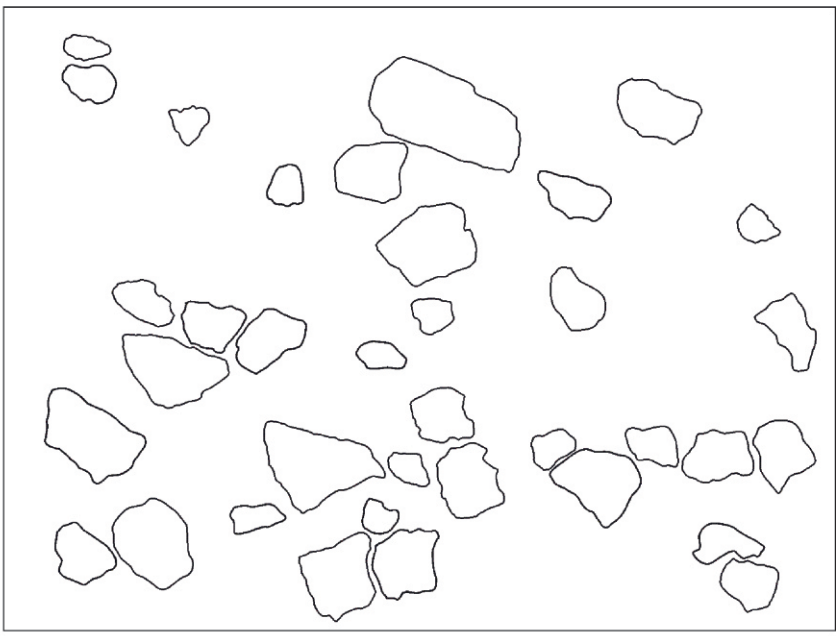

(C)

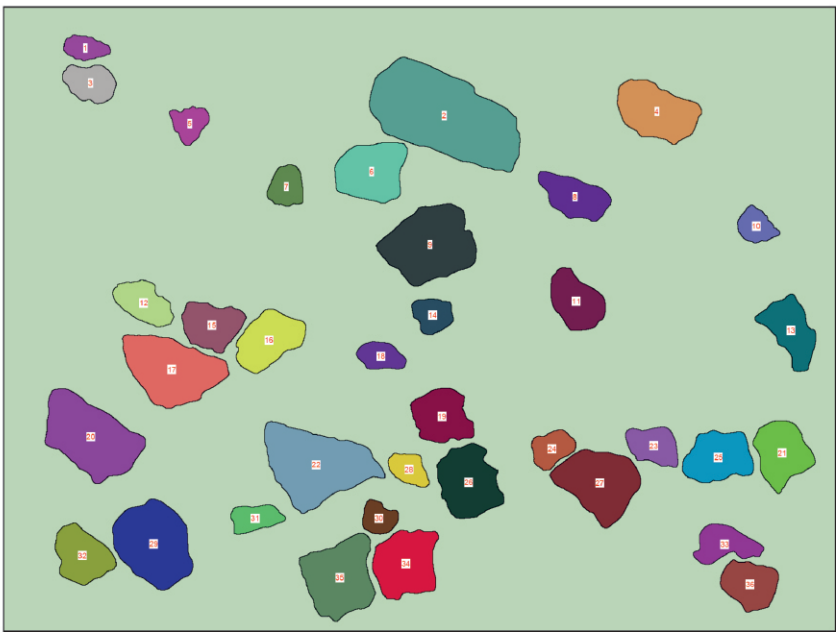

Figure 3

(A)

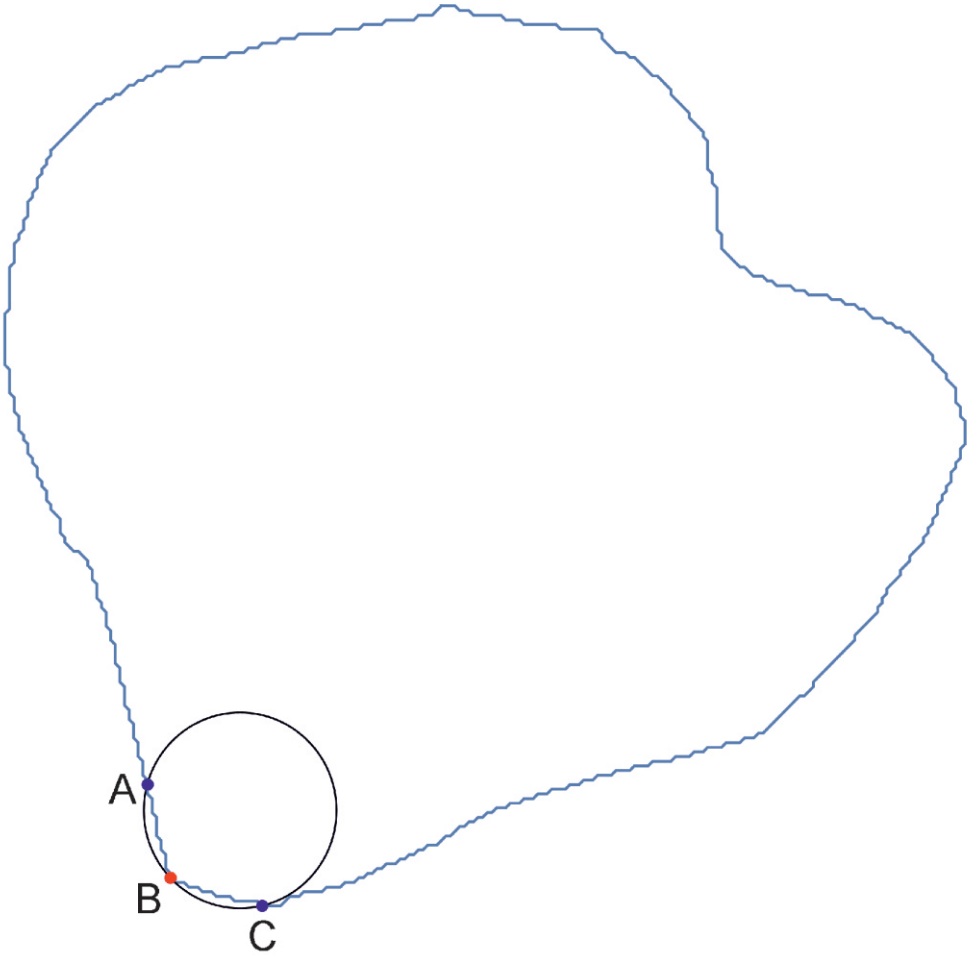
A
B
C

(B)

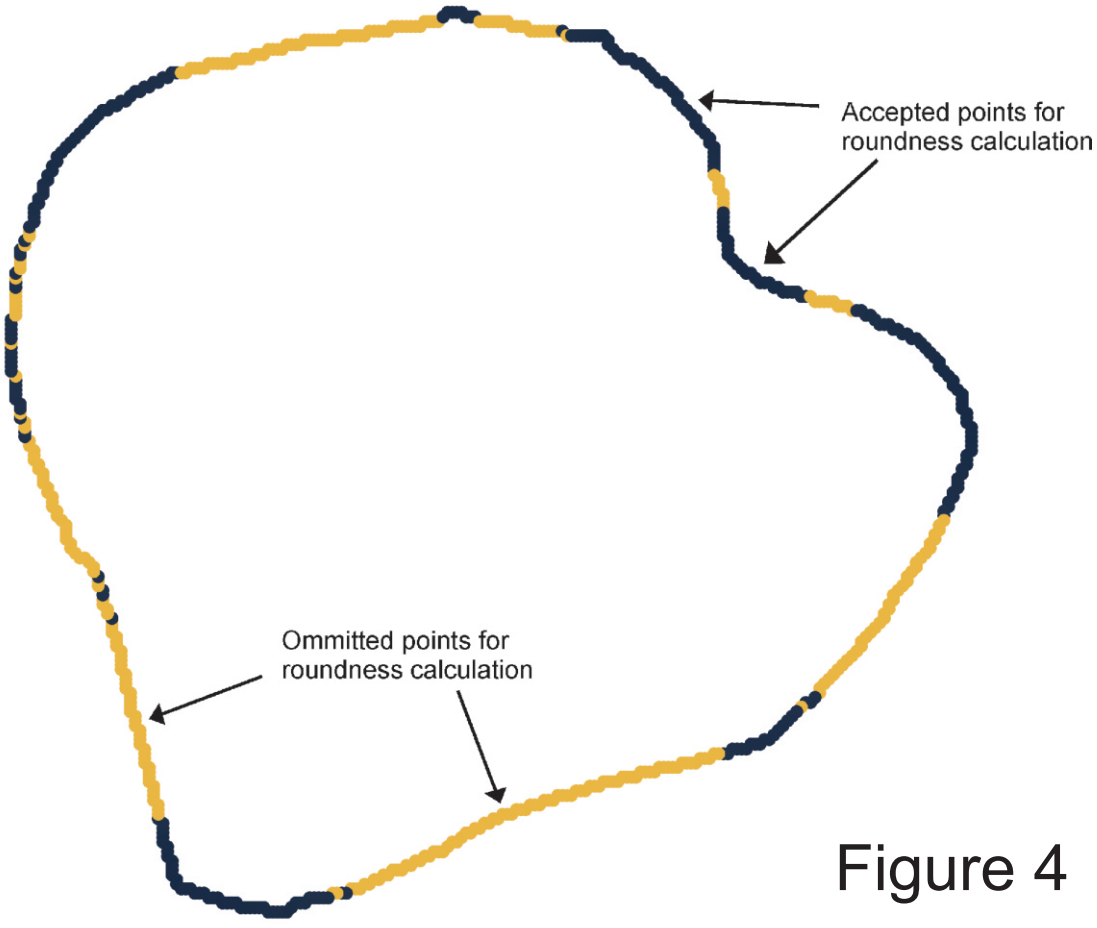
Accepted points for
roundness calculation
Ommitted points for
roundness calculation

Figure 4

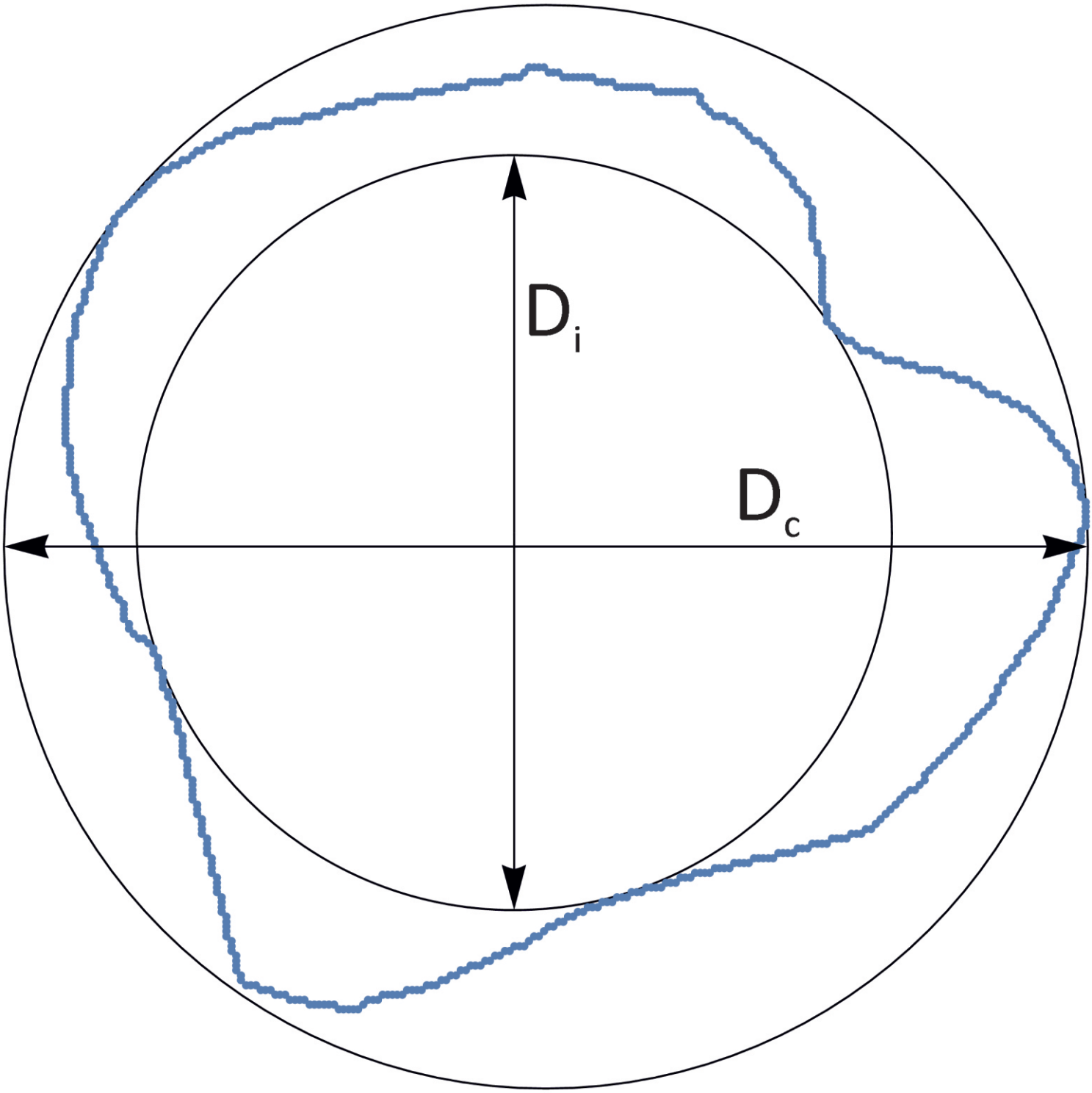

Figure 5

(A)

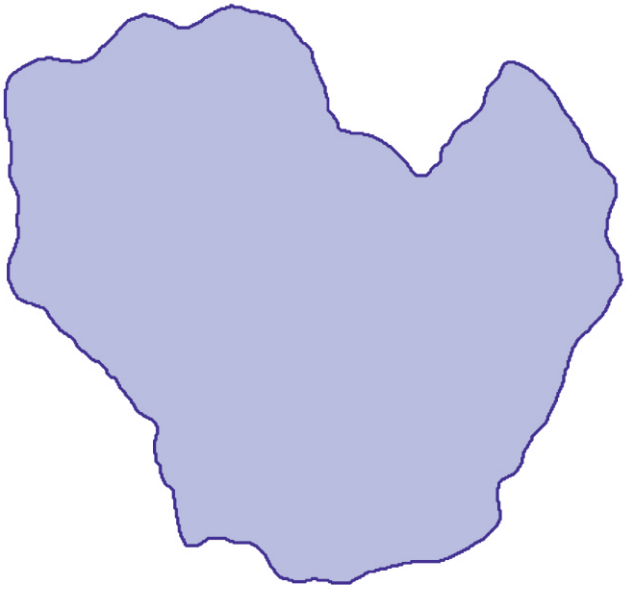

(B)

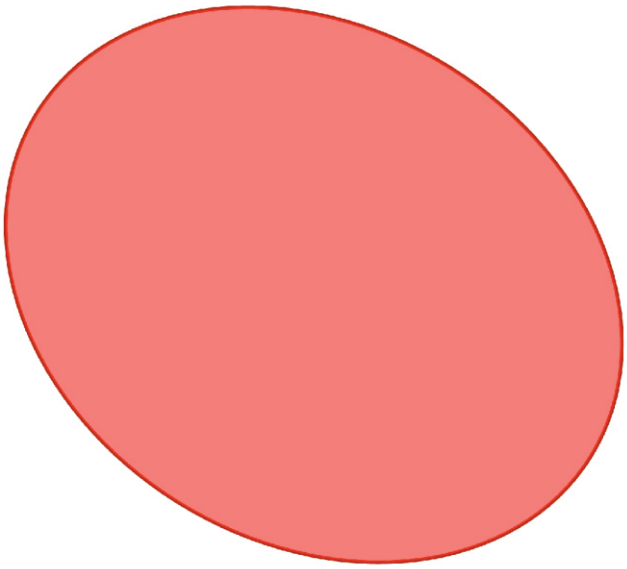

(C)

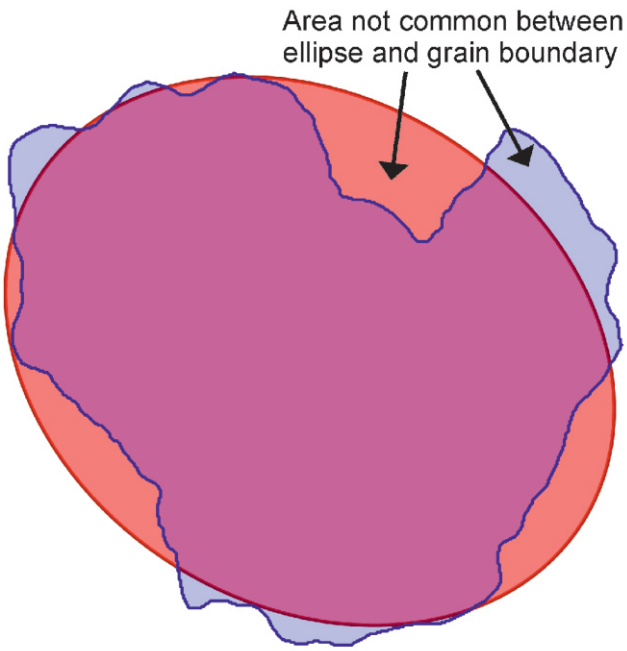

Figure 6

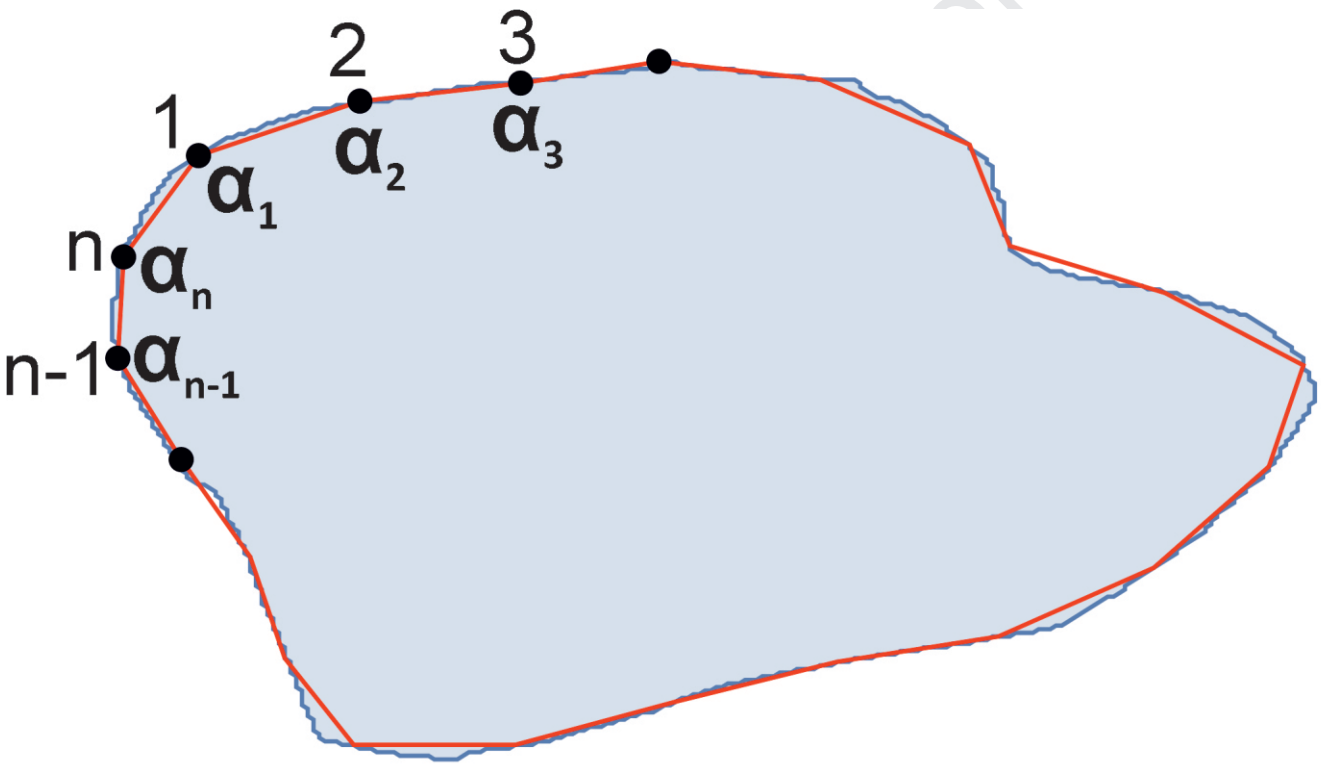

Figure 7

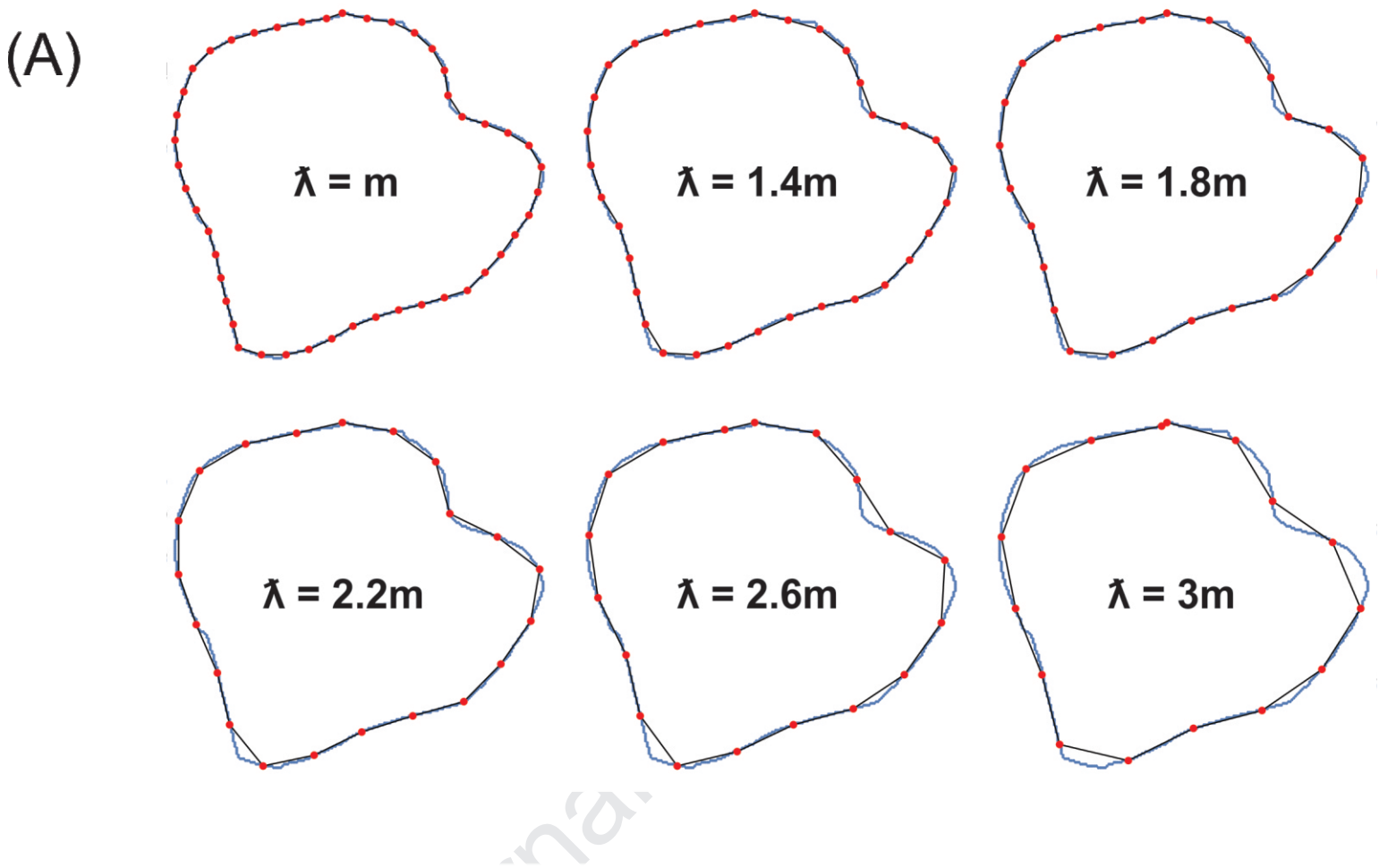
(A)
ƛ = m
ƛ = 1.4m
ƛ = 1.8m
ƛ = 2.2m
ƛ = 2.6m
ƛ = 3m

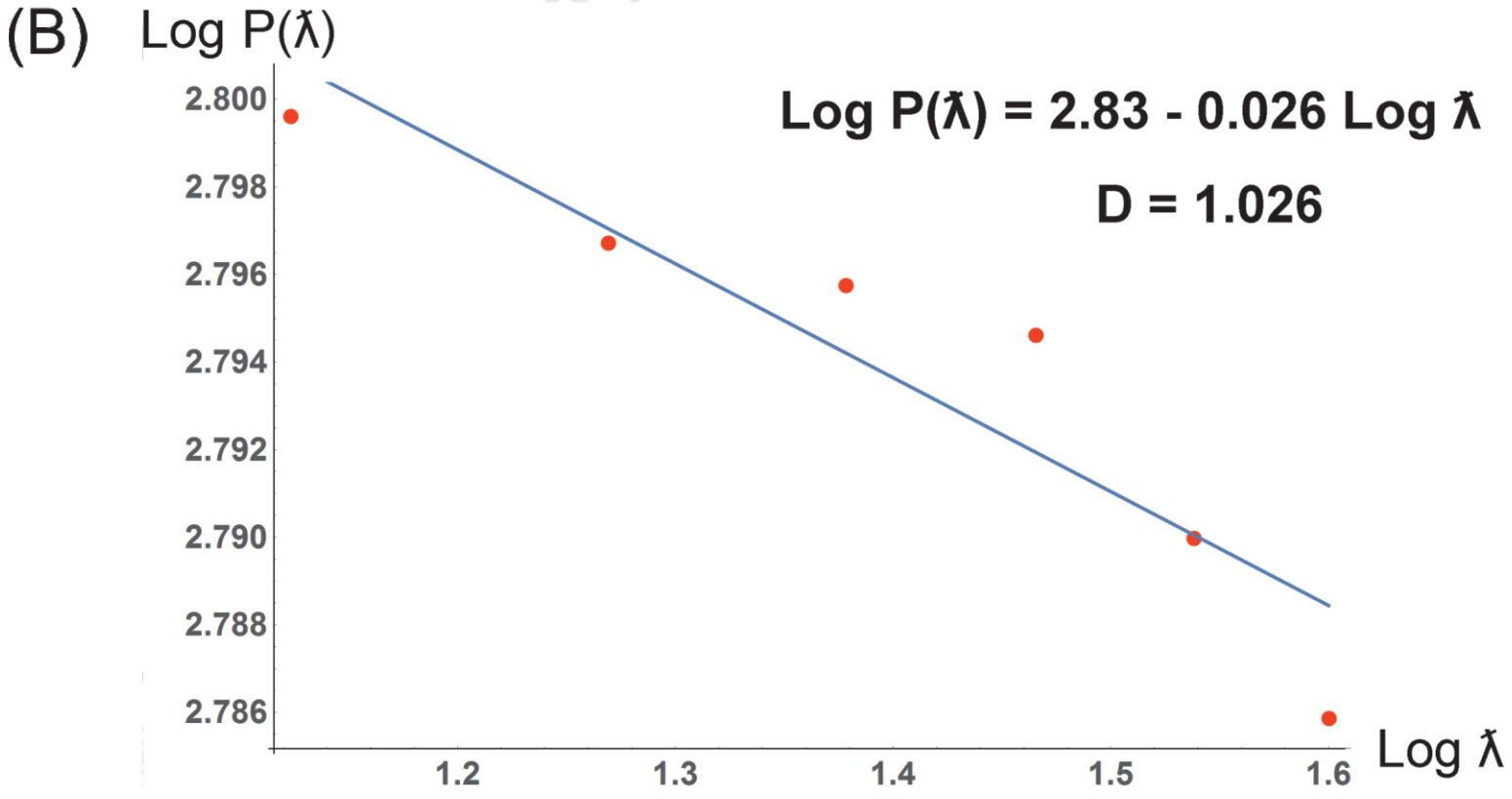
(B)
Log P(ƛ)
Log P(ƛ) = 2.83 - 0.026 Log ƛ
D = 1.026
2.800
2.798
2.796
2.794
2.792
2.790
2.788
2.786
1.2
1.3
1.4
1.5
1.6
Log ƛ

Figure 8

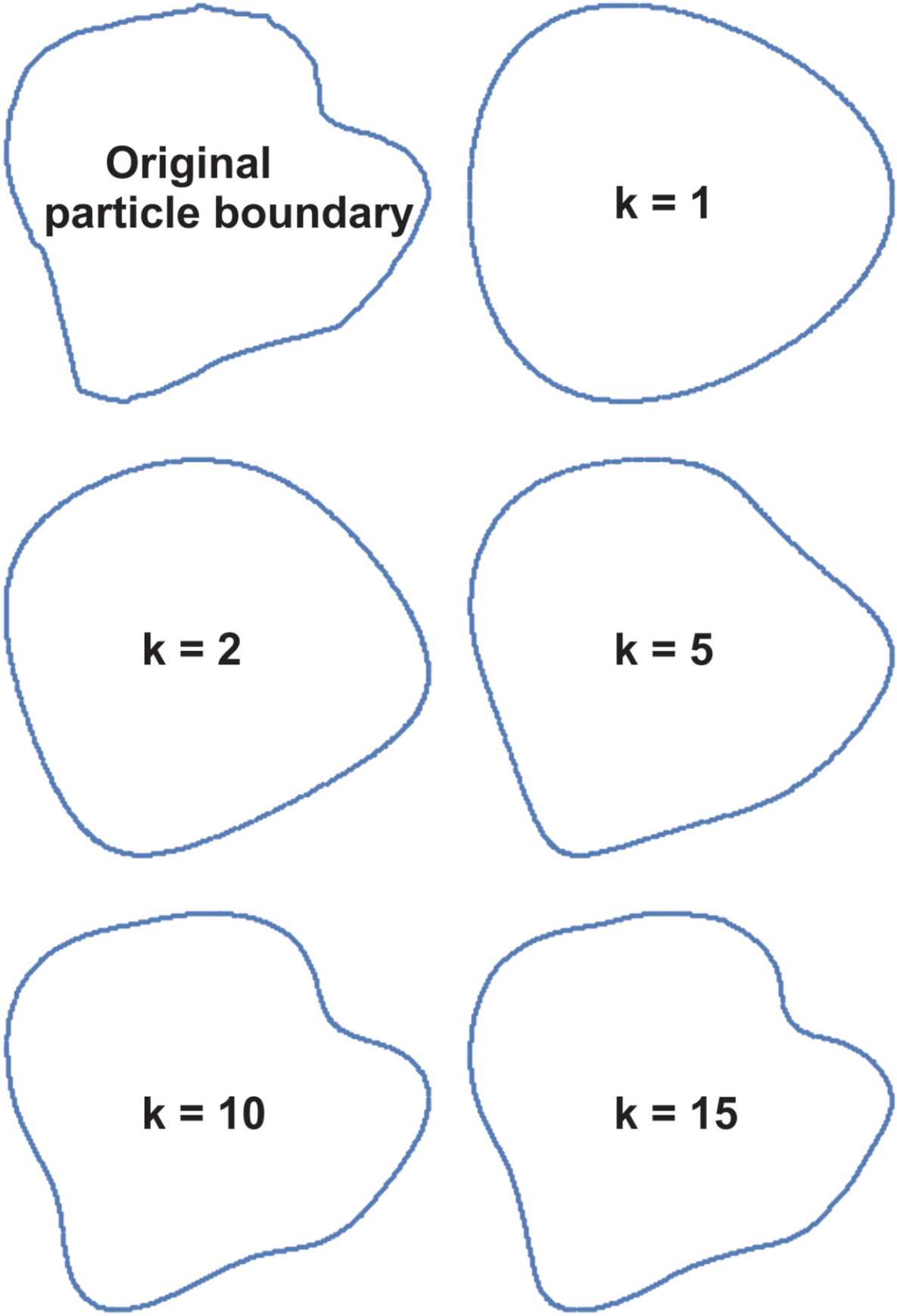

Figure 9

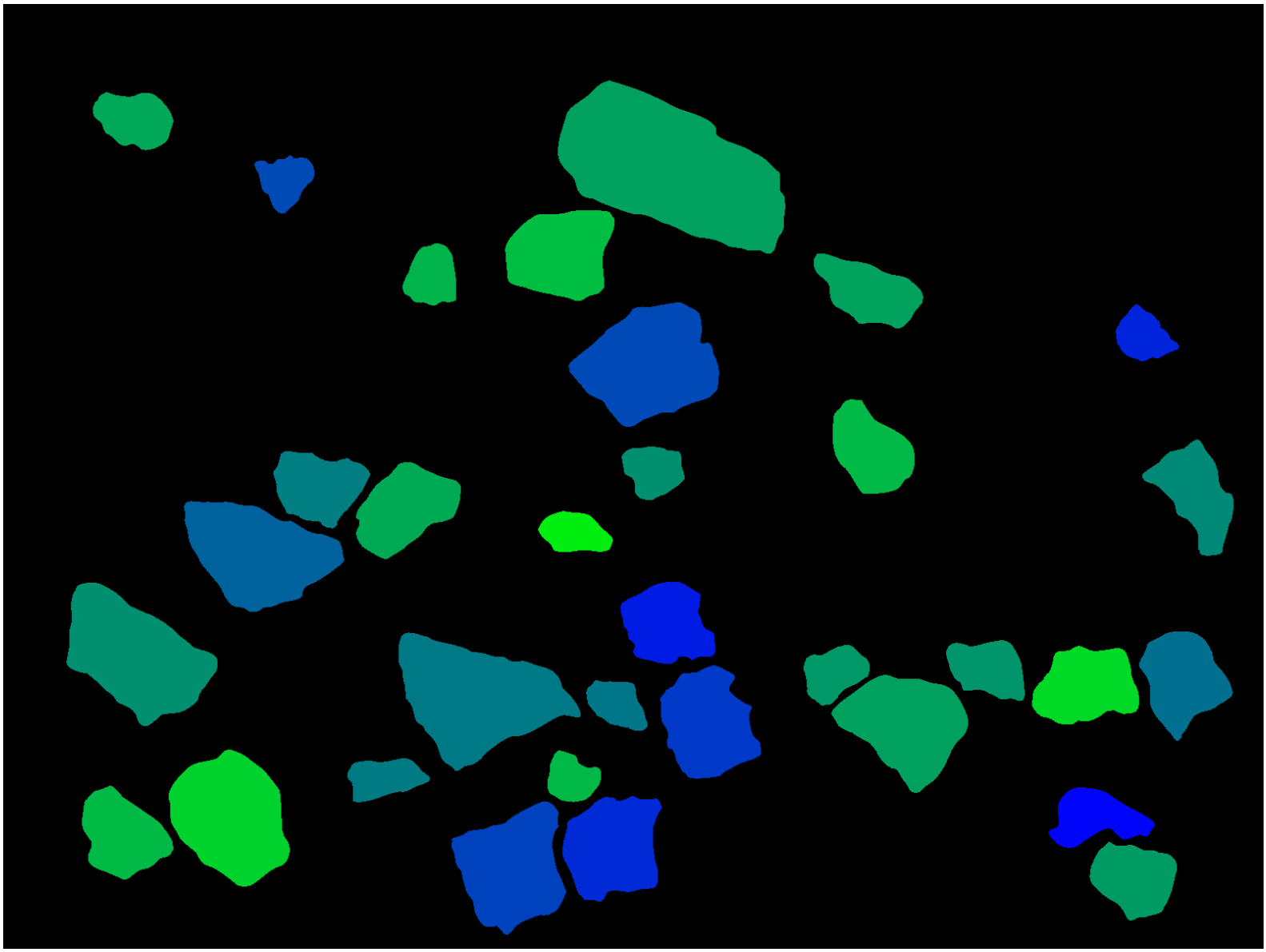

Figure 10

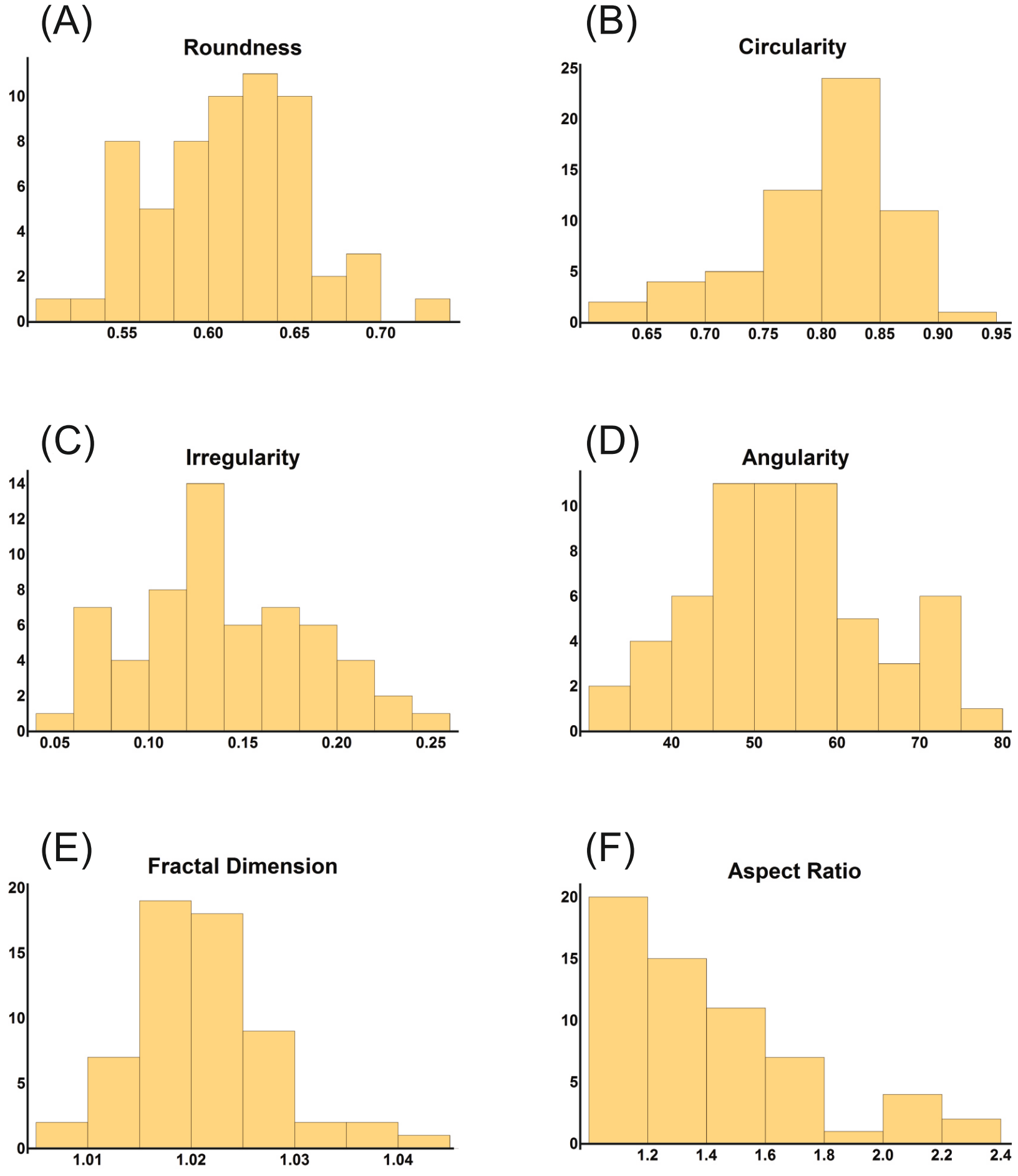
(A)
Roundness
0
2
4
6
8
10
0.55
0.60
0.65
0.70
(B)
Circularity
0
5
10
15
20
25
0.65
0.70
0.75
0.80
0.85
0.90
0.95
(C)
Irregularity
0
2
4
6
8
10
12
14
0.05
0.10
0.15
0.20
0.25
(D)
Angularity
0
2
4
6
8
10
40
50
60
70
80
(E)
Fractal Dimension
0
5
10
15
20
1.01
1.02
1.03
1.04
(F)
Aspect Ratio
0
5
10
15
20
1.2
1.4
1.6
1.8
2.0
2.2
2.4

Figure 11

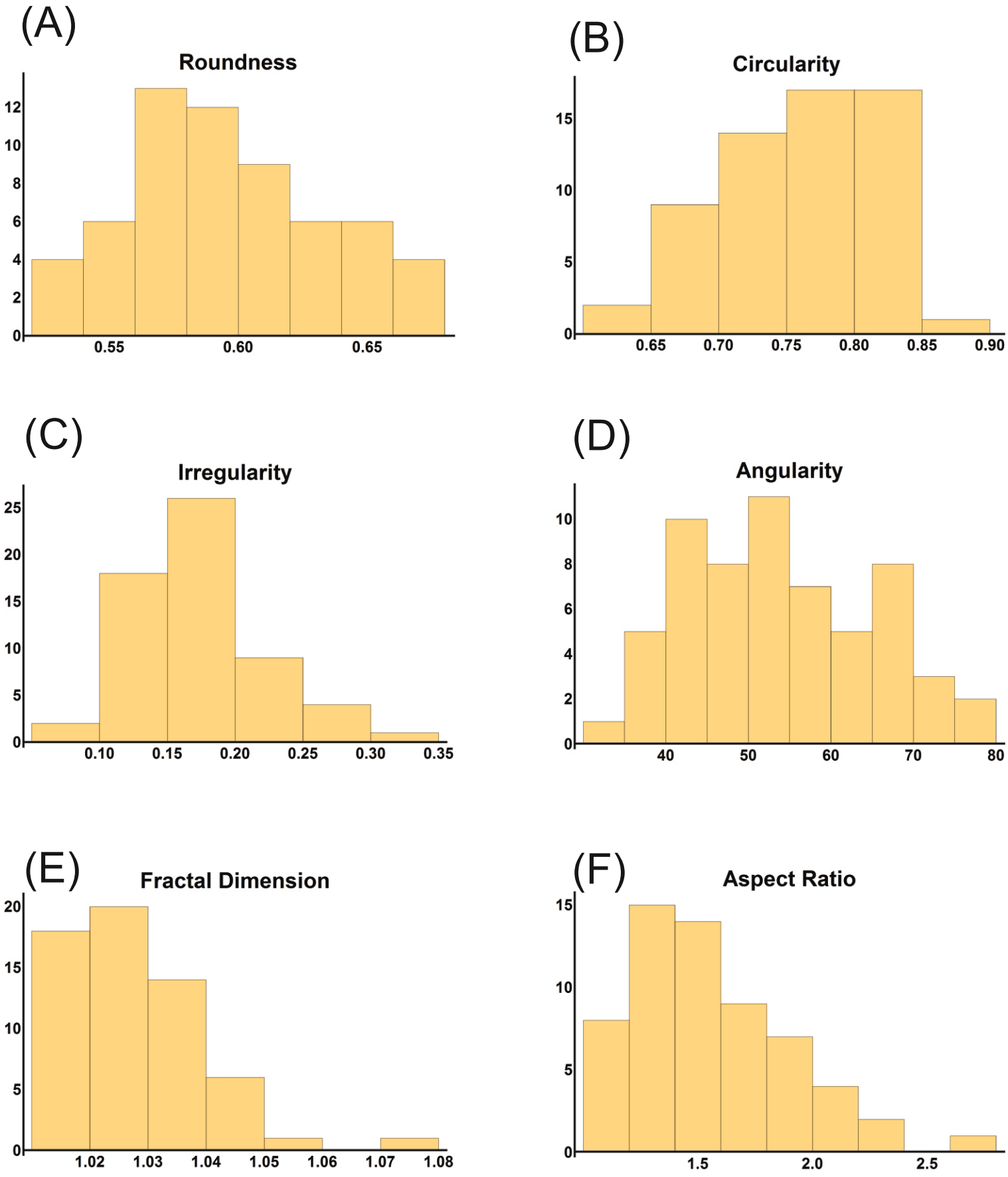
(A)
Roundness
0
2
4
6
8
10
12
0.55
0.60
0.65
(B)
Circularity
0
5
10
15
0.65
0.70
0.75
0.80
0.85
0.90
(C)
Irregularity
0
5
10
15
20
25
0.10
0.15
0.20
0.25
0.30
0.35
(D)
Angularity
0
2
4
6
8
10
40
50
60
70
80
(E)
Fractal Dimension
0
5
10
15
20
1.02
1.03
1.04
1.05
1.06
1.07
1.08
(F)
Aspect Ratio
0
5
10
15
1.5
2.0
2.5

Figure 12

Conflict of Interest statement

Date: 26-09-2019

Manuscript Code: CAGEO_2019_508

Manuscript Title: Image based Particle Shape Analysis Toolbox (IPSAT)

The authors listed below certify that they have NO affiliations with or involvement in any organisation or entity with any financial interest (such as honoraria; educational grants; participation in speakers' bureaus; membership, employment, consultancies, stock ownership, or other equity interest; and expert testimony or patent-licensing arrangements), or non-financial interest (such as personal or professional relationships, affiliations, knowledge or beliefs) in the subject matter or materials discussed in this manuscript.

Authors names:

Mohit Tunwal

Kieran F. Mulchrone

Patrick A. Meere